International Journal of Ambient Energy

ISSN: 0143-0750 (Print) 2162-8246 (Online) Journal homepage: https://www.tandfonline.com/loi/taen20

Computational Fluid Dynamics Investigation on Frictional Heat Transfer Flow process by using Fluid Method

R. Ramesh Kumar, J.M. Babu & R. Varatharajan

To cite this article: R. Ramesh Kumar, J.M. Babu & R. Varatharajan (2019): Computational Fluid Dynamics Investigation on Frictional Heat Transfer Flow process by using Fluid Method, International Journal of Ambient Energy, DOI: 10.1080/01430750.2019.1670259

To link to this article: https://doi.org/10.1080/01430750.2019.1670259

Accepted author version posted online: 19 Sep 2019.

Publisher: Taylor & Francis & Informa UK Limited, trading as Taylor & Francis Group

Journal: *International Journal of Ambient Energy*

DOI: 10.1080/01430750.2019.1670259

Computational Fluid Dynamics Investigation on Frictional Heat Transfer Flow process by using Fluid Method

RAMESH KUMAR.R[1*] J.M. BABU[2] R.VARATHARAJAN[3]
1,2,3 Department of Mechanical Engineering,
Vel Tech Rangarajan Dr.Sagunthala R & D Institute of Science and Technology,
400 Feet Outer Ring Road Avadi, Chennai, Tamil Nadu, India.
* ramesh.mech37@gmail.com

Abstract

The procedure of grating welding interfaces two strong state materials with a solitary strong with great holding joints. Consistent activities manufacturing weight with bit by bit utilized rotational drives joining the CFD comparable and different material procedure. Utilized for erosion weight, manufacturing weight, grating time, pivot speed, upset time, these frictional joints. Low information heat, short process duration and heat-affected areas were researched in this joining characters. This exploration work has created nonlinear models of three-dimensional limited components. The product was done ansys CFD workbench has been utilized to anticipate with results the thermomechanical heat generation investigation With numerical models and arrangements, test results were created. In this outcomes were created by heat affected zone and softening zone through the temperature distinction with mass disfigurements. Erosions welding of Ti-6AL-4V and SS304L Joints parameter results were built up fiction time is 5 sec, the pivot speed is 2100 RPM, contact weight is 80MPA and fashioning weight is 84.5MPA has been performed using CFD.

Keywords: CFD, finite element analysis, frictional heat transfer, temperature distribution, ambient energy and fluid flow.

Introduction

Divergent materials of weld uses are more in mechanical applications and car fields. Titanium and treated steels are high material attributes and great holding conditions in modern applications and aviation applications. Erosion welding process has great holding approach of strong to strong joining development [8]. In rubbing process, titanium bar has been fixed in revolution side and tempered steels are fixed in the non-pivot side. The turn side begins to pivot with certain RPM while non-revolution side devices are steady in the machine. Slowly expanding in RPM in revolution side the temperature additionally makes some purpose of grating with the non-pivot territory. At first begins the blaze purpose of under the connected weight; it achieved the plastic zone [1-3].

Heat is exchanged from mechanical vitality into warm vitality of the uniting procedure with under producing weight. In this exploration work concentrated on frictional parameters process with various fashioning weight and speed [4,6]. Consistent drive process is associating two strong materials with joining parameters. This welding procedure to deliver low heat information and vitality spares with mechanical applications [4-7]. In contact welding procedure could be utilized to weld bar to bar, bar to pole and so on. Two unique stages are delivered in the grating welding process. One is a heating stage and another is disquieting stage [5]. The heating stage follows up on contact between the turn and non-pivot side poles with shifting weight. This connected weight is called as heating weight.

Time taken for acts in weight in the welding procedure is known as a heating time. The second phase of irritating weight is constrained by weight. In this stage, materials are connected with expanding weight with contact area [7]. In thermo-mechanical procedure follows up on the pole, it disfigured and diminished with its unique length. The

procedure of weld arrangement is created by material quality and welding quality [10]. On account of different material joining quality extends the warm coefficient and material hardness expanded with relies upon the weight ranges [8-9].

This warm coefficient of titanium and treated steels are grown correspondingly 32.8 and 9.4 μm/^{O}C. The hardened steel and titanium work piece distances across are independently 16mm. The work piece could be turned at 1600-2300 rpm for each second it follows up on the great bond among titanium and treated steel [11]. This case steadily expanding in compelling weight it exhibitions 158-171 MPa in beneath of 2 seconds in welding conditions.

In this momentum inquire about work clarified about the highlights of improvement factors on quality of weld, heat exchange rate, heat motion coefficient, heating time and miss happening of proportional worry for the term of unsurprising rubbing welding of Ti-6AL-4V and SS304L [19]. This exploration work was overviewed under different places of manufacturing weight, frictional time, rotational speed and frictional weight.

Table 1 Ti-6AL-4V (grade 5) Thermal Properties

Property	**Value**
Density g/cm^3 (lb/ cu in)	4.42 (0.159)
Melting Range °C±15°C (°F)	1649 (3000)
Specific Heat J/kg.°C (BTU/lb/°F)	560 (0.134)
Thermal Conductivity W/m.K (BTU/ft.h.°F)	7.2 (67)
Mean Co-Efficient of Thermal Expansion 0-100°C /°C (0-212°F /°F)	8.6x10^{-6} (4.8)
Mean Co-Efficient of Thermal Expansion 0-300°C /°C (0-572°F /°F)	9.2x10^{-6} (5.1)

Table 1 represents the Thermal properties of Ti-6AL-4V (grade 5) and its values.

Table 2 SS304L Thermal Properties

Property	**Value**
Density	0.284 lbs./cu.in.
Melting Point	1400° C
Electrical Resistivity @ R.T	72 Microhm· cm
Thermal Expansion Coefficient (0° to 100° C)	17.3 x 10-6/ °C
Thermal Conductivity @ 100° C	16.3 W/m· K

Table 2 represents the Thermal properties of SS304L and its values.

2. Mathematical Formation

Coulomb's law dependent on an erosion welding process is chipping away at contact pressure and connected weight. In scientific development shear pressure performing on the rubbing welding process, conditions are given in condition number1

$$\tau_f = \mu P \tag{1}$$

Shear stress mathematical notation is τ_f, the coefficientof friction is μ, and axial pressure notions are formed in P.

Frictional coefficient [13] the revolution stream is regularly exchanging heat starting with one pole then onto the next bar. Higher temperature makes pressure flow of grinding region induced shear pressure adjusted by Coulomb's law [3].

$$\tau_{shear} = \tau_f = \frac{\sigma_s}{\sqrt{3}} \tag{2}$$

Stream shear pressure numerical documentation in CFD is, identical stream worry in fea documentation is Coulomb's law clarified the shear stream rate with pivotal weight.

$$Q = \eta * \gamma * \tau_f = \eta * \gamma * \min(\mu P, \frac{\sigma_s}{\sqrt{3}}) \tag{3}$$

Heat generated equation of friction welding continuous drive process are shown in equation number (4)

$$Q = \delta * \eta * \gamma * \mu * P + (1-\delta) * \eta * \gamma * (\frac{\sigma_s}{\sqrt{3}}) \tag{4}$$

Q is the heat generated rate, δ is a sliding fraction, η is a heat efficiency, γ is a slipping rate of friction, μ is the friction coefficient. Heat generated process which makes the mathematical operations occurs in finite element methods for friction process.

Heat transfer mathematical modeling formulas are derived from Fourier heat conduction equations [4].

$$k\left[\frac{\partial^2 T}{\partial x^2} + \frac{\partial^2 T}{\partial y^2} + \frac{\partial^2 T}{\partial z^2}\right] + Q = \rho C_p \frac{\partial T}{\partial t} \tag{5}$$

From this equation, k is the thermal conductivity, T is the temperature distribution, ρ is the density of materials, C_p is the specific heat. This modeling produces the heat transfer rate value and temperature distribution values [4].

$$f = \frac{\sqrt{(k\rho C_p)_{workpiece}}}{\sqrt{(k\rho C_p)_{workpiece} + (k\rho C_p)_{total}}} \tag{6}$$

f is the split ratio of the material deformation process, k is the thermal conductivity, ρ is the density of materials, C_p is the specific heat, subscripts are showing workpiece and tool for material properties.

Zorev's computational friction method [7] was implemented to overcome Coulomb's law to reduce friction time and increasing contact regions.

$$\tau_f = \begin{Bmatrix} \tau_p : \mu\sigma_n \geq \tau_p, (l_p < x < l_c) \\ \mu\sigma_n : \mu\sigma_n < \tau_p, (0 < x < l_p) \end{Bmatrix} \tag{7}$$

τ_f is the parameter frictional stress, σ_n is the normal stress, μ is the friction coefficient of region frictional contact, l_p is the sticking zone, l_c is the sliding zone.

Two solid connection models were developed with heat flux friction with transfers the heat increasing rate [10].

$$h_{tc} = \frac{d}{dA}\left(\frac{dQ}{dt}\right) \tag{8}$$

h_{tc} is the thermal conductance of the contact method, A is the contact surface, Q is the heat flux rate.

3. COMPUTATIONAL FLUID DYNAMICS MODELING

Computational fluid dynamics methods are created by different limit conditions with assistance of warm stream issues and great holding areas. Ansys programming finds the warmth flex and expanding temperature areas on various preliminaries. Warm stream parameters to examination with assistance of Ansys transient warm investigation with typical conveyance loads [11]. In this simulation, thermo mechanical limit esteem issues are picked and examinations with steady weight and speed. The CFD thermal properties are appeared table 2.

3.1. Geometry & Meshing

CFD workbench draws a three-dimensional model with the elements of 16mm distance across and 50mm length of two roundabout bars [18, 7]. These two bars are reached with grinding contact area and typical weights. This is thinking about to mechanical and warm properties to play out the recreations. Ansys coinciding elements are demonstrated to better quality of elements with holding. Fine work utilizing element size of bended surfaces with edges is all around reinforced [12]. Tetrahedron work element was received to discover the quality of the finite element strategy and materials quality. At first, course work calculations work in geometry. In any case, some resilience was not acknowledged in the cross section conditions, so we changed the fine work with estimating are picked 2mm and fit surface cutoff points are acknowledged under as far as possible. Last acknowledged work hubs are 12,512 and elements are 40,832. The uncommon tirelessness elements coincided with contact surfaces between two round bars. Limit conditions are connected one end is fixed and opposite end conveys connected weight with rotational speed. Removals are captured with the x and y headings. Conduction, convection, radiation procedure could be considered to apply the warm limit stages. Finished coincided with geometry is appeared in fig 1.

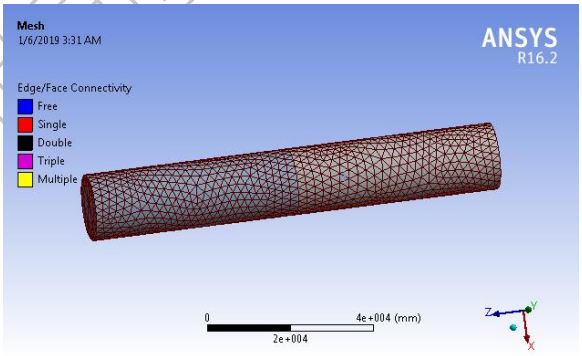

Fig 1 Meshed 3-D CFD Model of Ti-6AL-4V and SS304L

3.2. Boundary conditions

The two round bars after coincided with connected the limit conditions. It has two zones. One is Rotation zone and another is non-Rotation zone. Non-pivot zone was fixed with all directions. The rotational zone was connected weight with certain speed and removal was connected in x and y arranges. In this condition, z facilitates move with uninhibitedly shown in fig 2.

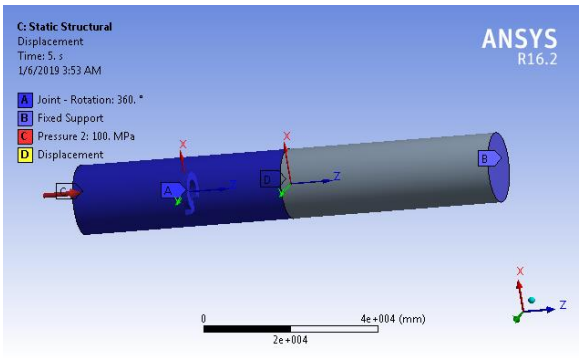

Fig 2. Applied CFD Boundary Conditions

3.3. Material Conditions

Johnson-cook model has built up the thermo mechanical investigation with typical anxiety rate. The warm class comprises of the plastic and flexible district of nonlinear examination with room temperature and liquefying temperature. The material model was utilized by Johnson-cook law. The most extreme pressure incited in grating welding process which influences in limit conditions in the material procedure. Temperature zone esteems are determined in the softening stage and warmth exchange zone is composed by[9]

$$\sigma = (A + B\varepsilon^{n})\left[1 + C\ln\left(1 + \frac{\dot{\varepsilon}}{\dot{\varepsilon}_0}\right)\right]\left(1 - \left[\frac{T - T_{room}}{T_{melt} - T_{room}}\right]^{m}\right) \tag{9}$$

σ Is the pressure stream work, A & B are constant material melding points, C is the combination of materials, ε is the strain, $\dot{\varepsilon}$ is the strain rate, $\dot{\varepsilon}_0$ is the reference strain rate, T_{melt} is the dissolving temperature, T_{room} is the room temperature of warmth streams.

3.4. CFD Simulation Setup

Static basic and transient warm investigation reenactment execution results are done by complete distortion, comparable pressure, ordinary pressure, shear pressure, most extreme and least pressure. In this exploration work includes in nonlinear examination with mass distortion stresses inciting in hub weight [15]. A heap period comprises of keeping up annoying time and warming time. Ansys highlights of programmed time setting keep up the reenactment parameters and time.

Table 3 CFD setup for friction process

S.No	Friction Pressure	Friction Time	Forging Pressure	Forging Time	Speed (RPM)
1	40	5	40	5	1600
2	40	5	40	5	1800
3	50	5	50	5	2000
4	60	5	60	5	2400
5	90	5	90	5	2400
6	70	5	70	5	2200

4. Results and Discussion

In this exploration work includes in recreation process for nonstop drive capacity of erosion welding parameters like producing weight, annoying time, temperature. Exploratory outcomes were dissected with a numerical definition with connected limit conditions. These numerical outcomes came to close to the CFD test Results. Meshed views are shown in fig 3.

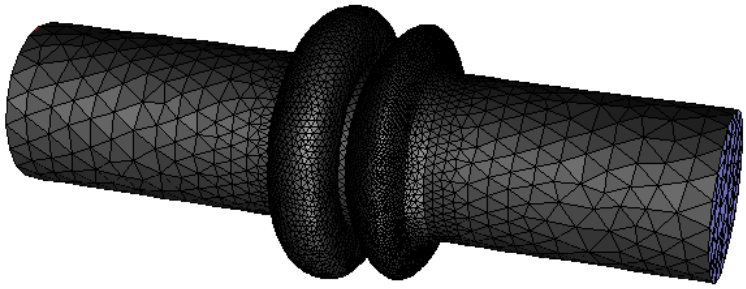

Fig 3. Sweep Meshed model for different materials

Rubbing welding temperature results are appeared table 5. Every one of the parameters is determined and happy with 85% certainty levels. In the parameter concentrate to examine the temperature difference with ordinary investigation state conditions are shown fig 4.

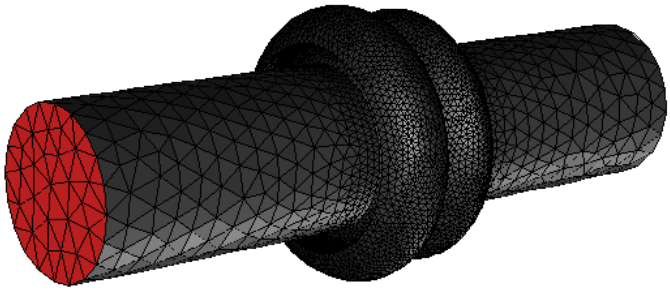

Fig 4. Nodal variation of meshed views

The plastic region material characteristics are deformed with constant pressure and rotating velocity. This deformation results are showing the fig .5 is maximum displacement levels. The maximum endurance force acting at 2470 N. This force endurance data is shown in fig 5.

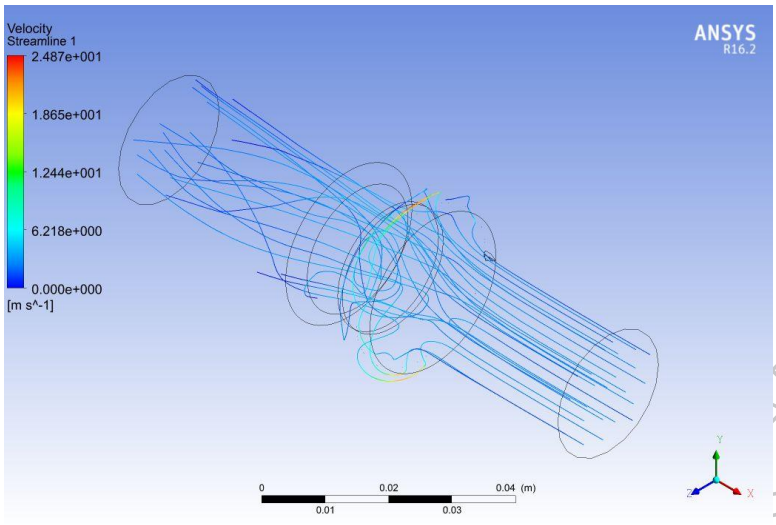

Fig 5. Velocity and temperature flow in CFD

The comparable qualities are determined with the utilization of the plastic area. These parameters are determined and demonstrated with 85% certainty levels. The most extreme key pressure is more than when contrasted with proportional pressure. These endeavors called as region exertion values are shown in fig 6.

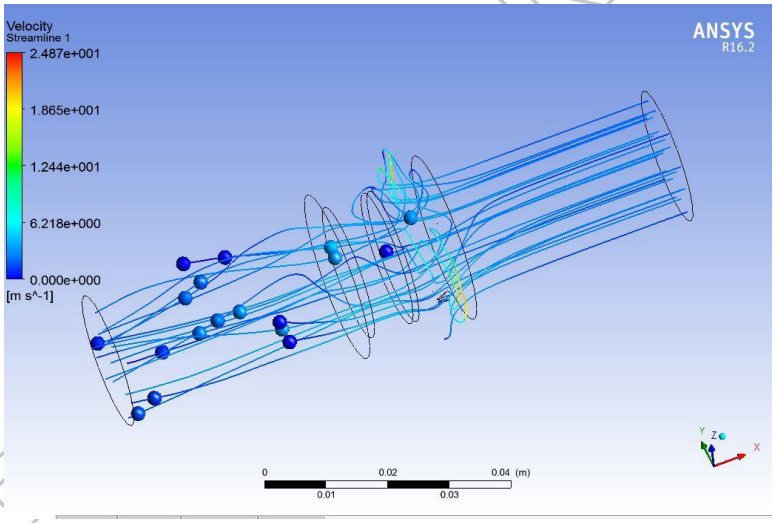

Fig 6. Velocity Streamline of CFD flows.

Proportionate pressure results are increasingly proficient for shear pressure comparable. In this friction, a procedure controlled the weight shifting from the first stage to distorted stages results are shown in fig 6.

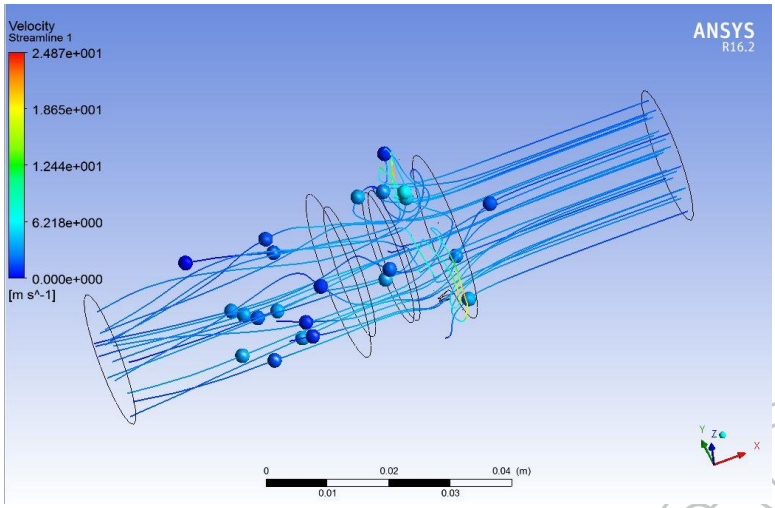

Fig 7. Time increment and time setup variance

The above setup result parameters are distinguished expanded time setup with consistent twisting of flexible plastic districts. Weight and rotational speed will progressively increment with a base of the time increase. The temperature inclination will blend two different material procedures. Proportional pressure focus levels are expanding with assistance of the typical time setup parameters are shown in fig 7.

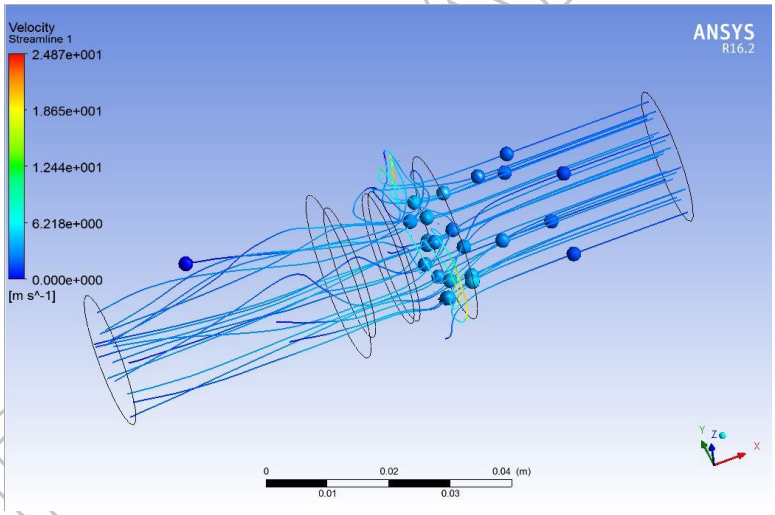

Fig 8. Time variance of CFD flow

Ti-6AL-4V and SS304L material blends influence the vitality loss of hourglass and contact vitality. A changing number of cycles acting at the steady weight and twisting stages are acted relies upon consistent CFD temperature results are shown in fig 8.

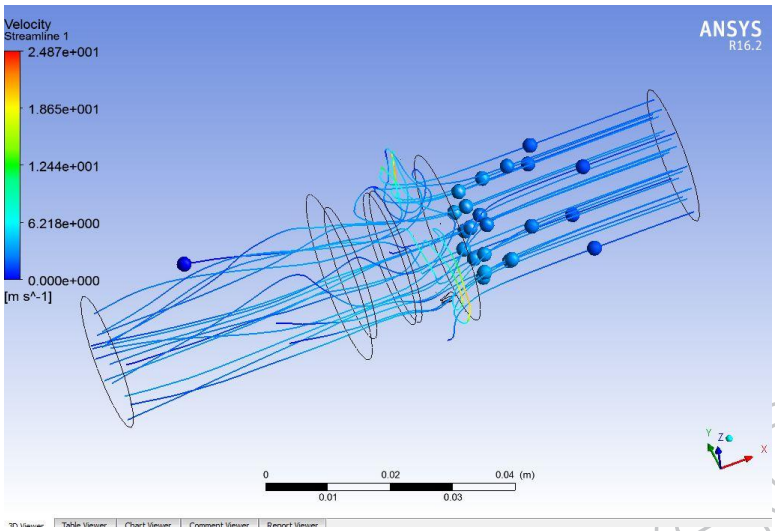

Fig 9. Velocity reaction on CFD flow process

Velocity stream flow process results are shown in fig 9. The deviations of temperature disturbance results are carried out from mathematical models and theoretical models.

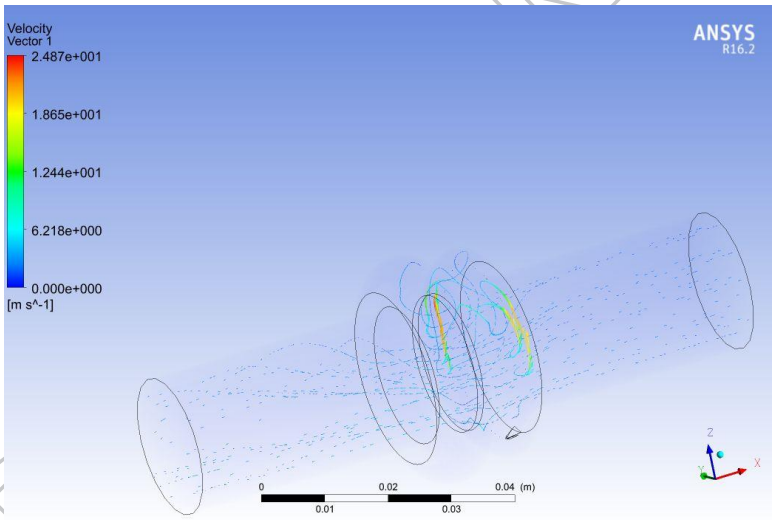

Fig 10 CFD vector path on inlet simulation

Frictional contact zone effects are constrained by weight with power. Rotational lengths are shifting by the speed of the speed movements are shown in fig 10, 11.

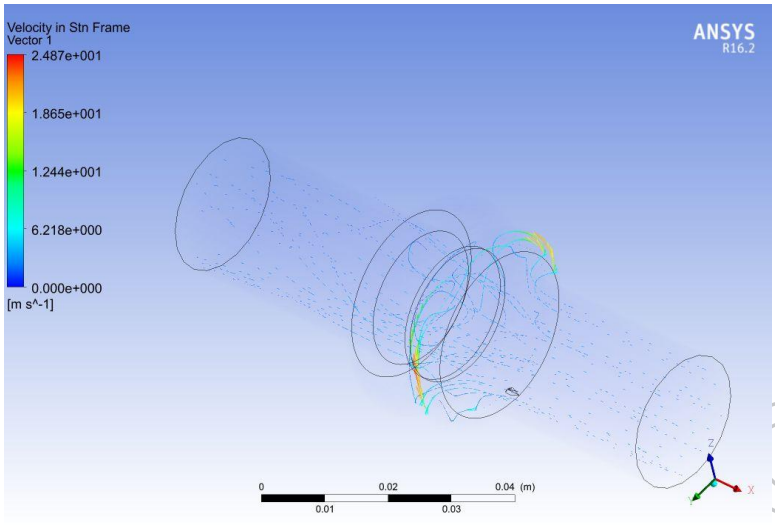

Fig 11. CFD vector path on outlet simulation

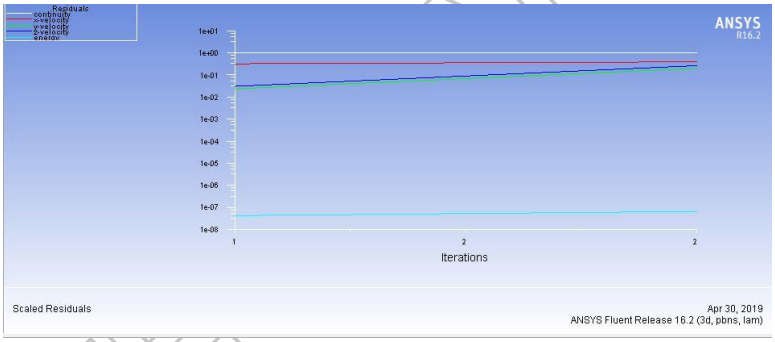

Fig 12. Incremental iteration of CFD process

Incremental iteration process results are carried out from analytical values shown in fig 12.

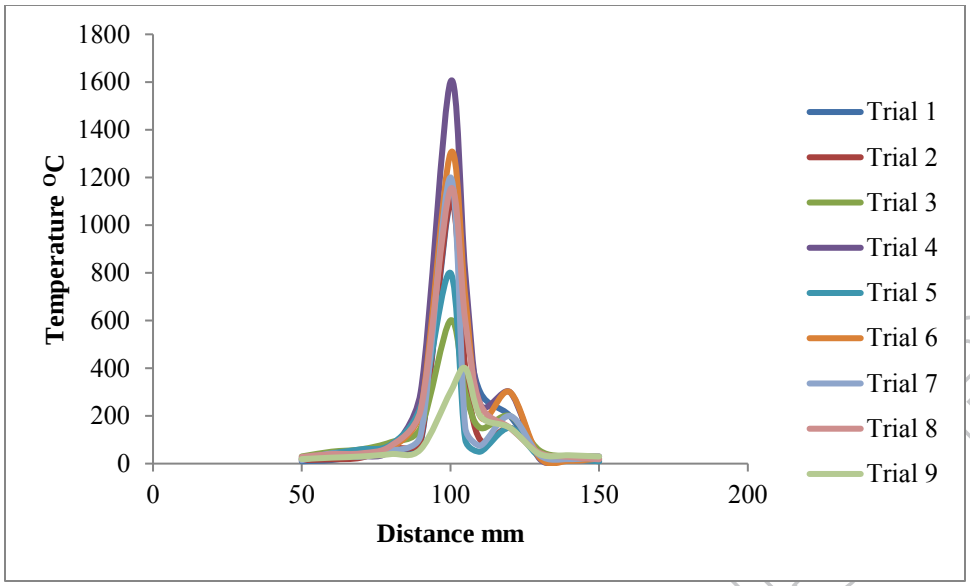

Fig 13. Distance vs. Temperature Results on CFD joining process

The plastic locales are progressively changed with distortion of fourth and fifth stages. This exertion is known as the time gradual procedure. Separation and temperature results are appeared in fig 13. This outcome is clarified about the joining of different materials and joining separation.

4.1 Energy loss in frictional process of CFD analysis method

Complete distortion is fundamentally spoken to for all directional worry with one of a kind quality. The all out twisting is essentially followed up on Ux, Uy, Uz directions. The trail 6 is appearing most extreme absolute miss happening a result with steady weight continuance constrains on beneath results. Critical parameter complete twisting outcomes are appeared in fig 14.

iter	continuity	x-velocity	y-velocity	z-velocity	energy
1	1.0000e+00	3.2130e-01	2.3458e-02	3.0544e-02	4.2909e-08
2	1.0000e+00	3.9244e-01	1.9977e-01	2.6334e-01	6.6040e-08
3	1.0000e+00	2.7120e-01	2.9347e-01	1.5337e-01	7.2192e-08
4	9.8641e-01	1.5093e-01	1.1936e-01	9.2505e-02	7.3274e-08
5	1.0000e+00	1.1260e-01	8.3517e-02	7.5026e-02	7.3465e-08
6	9.5516e-01	1.0094e-01	6.7120e-02	6.0600e-02	7.3561e-08
7	9.0597e-01	9.1110e-02	5.9261e-02	5.3348e-02	7.4513e-08
8	1.0039e+00	8.3373e-02	5.9010e-02	5.1437e-02	7.4404e-08
9	8.6057e-01	7.5141e-02	5.3013e-02	4.5752e-02	7.3793e-08
10	9.8802e-01	6.7443e-02	5.1523e-02	4.2786e-02	7.4810e-08
11	8.6453e-01	5.8384e-02	4.5901e-02	3.7495e-02	7.4458e-08
iter	continuity	x-velocity	y-velocity	z-velocity	energy
12	8.7038e-01	5.1278e-02	4.4325e-02	3.5346e-02	7.5525e-08
13	8.4577e-01	4.8669e-02	4.5670e-02	3.2148e-02	7.4511e-08

Fig 14. Total energy loss results on CFD process.

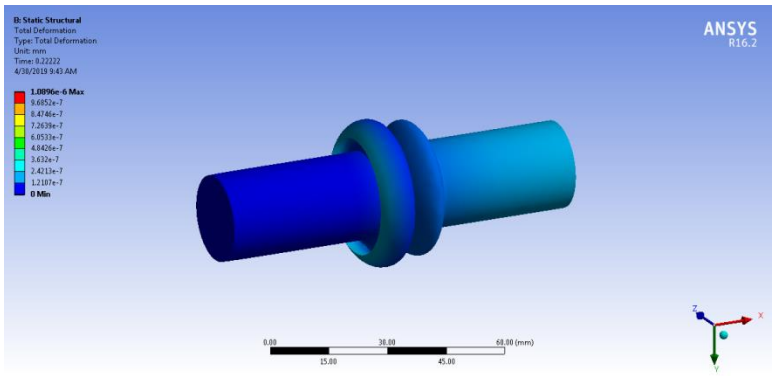

Fig 15. Initial Temperature variance on CFD

In this examination work examination of 4 tests with 9 set of preliminaries. This procedure could be distorted consistent shifting divisions of three distinct stages. The various arrangements of stages are appeared in fig 15 as beneath.

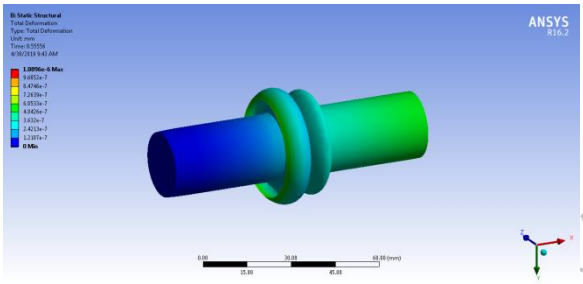

Fig 16. Normal Temperature Variance on CFD

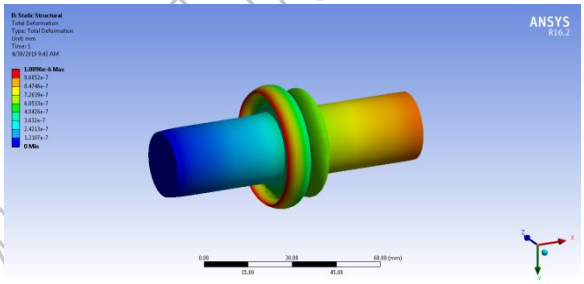

Fig 17. High temperature variance on CFD

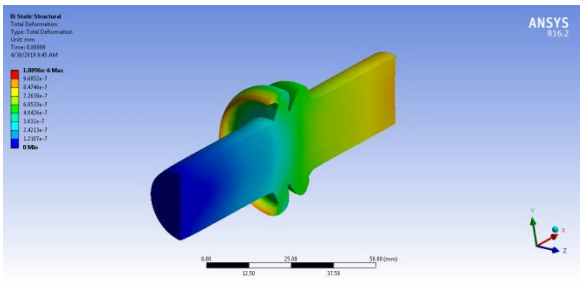

Fig 18. Cut Section view of CFD results

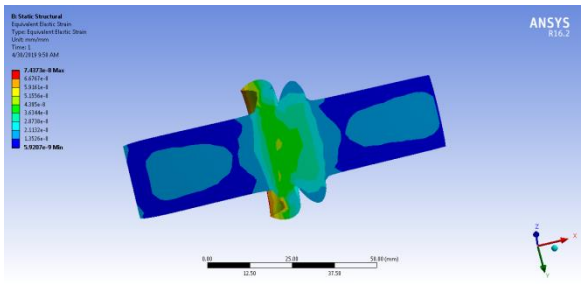

Fig 19. Frictional joined samples of CFD process

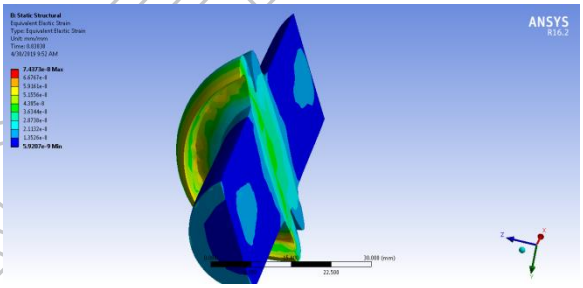

Fig 20. Section view of Frictional joined CFD process

The time steady setup was step by step expanded with assistance of various weights and fluctuating plan of getting distorted shapes. Preliminary 7 shows the most extreme variance of vitality put away with changes from versatile from

the plastic district. The controlled setup results investigate with assistance of Ansys CFD workbench graphical speaks to appeared in fig .16-20.

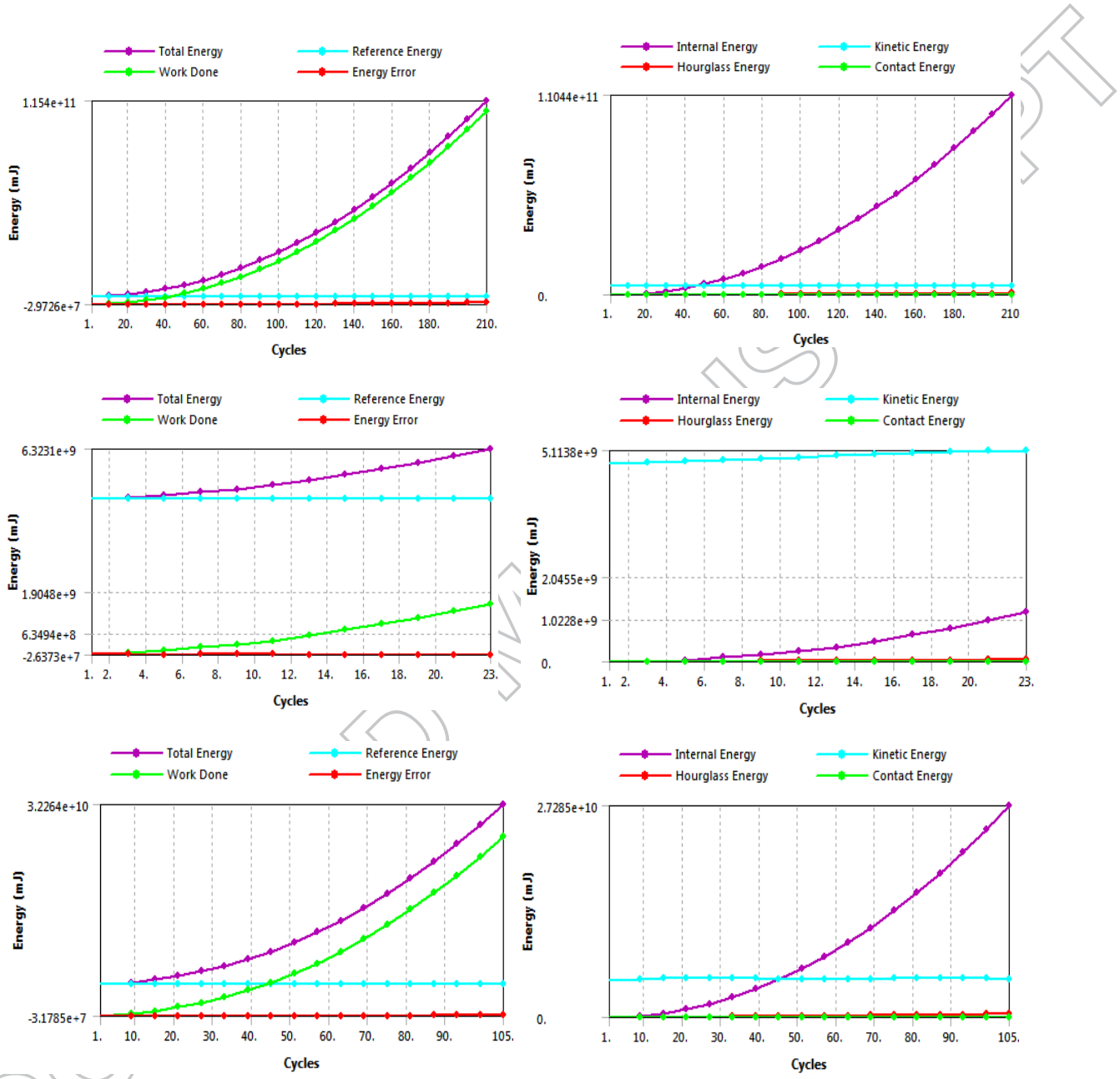

Fig 21. Number of cycle's vs. energy loss results analysis in CFD

Energy loss parameters are mentioning the above graphs to determine the natural convection on materials joining process in CFD. This temperature dispersion controls on various cycles with plastic deformation with the steady rotational speed of the distinctive arrangement of preliminaries are shown in fig 21.

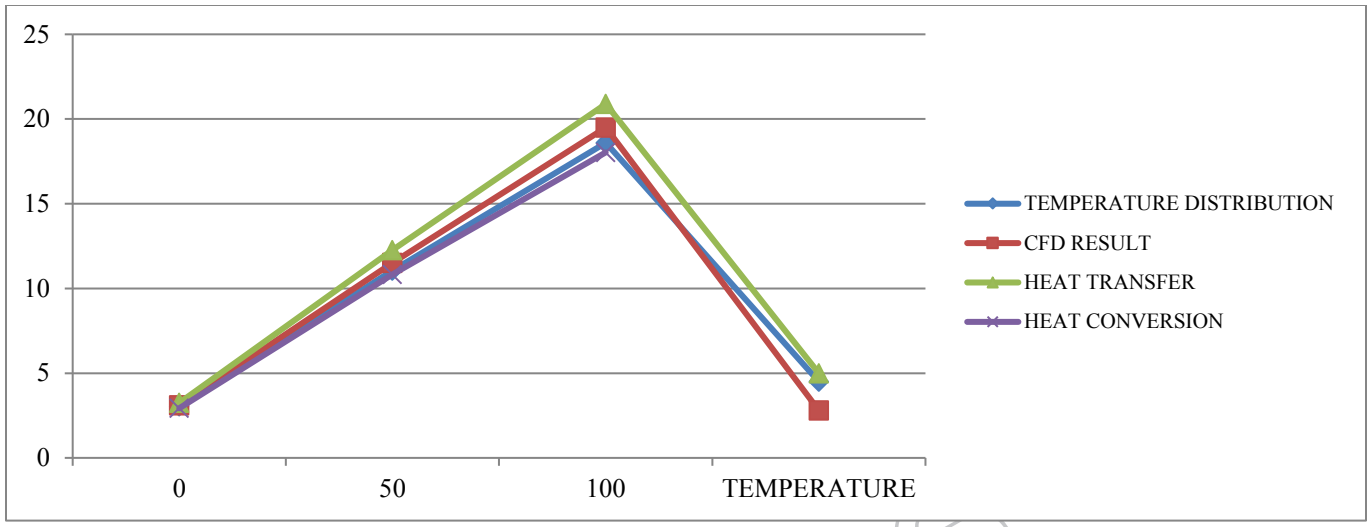

Fig 22. Temperature vs. pressure results are all method process

Pressure and temperature results are mentioned in the graphical formation shown in fig 22. The minute outcome ranges are expanding with consistent of 571.8, 2199.5, 8250, 17288 (N-s).

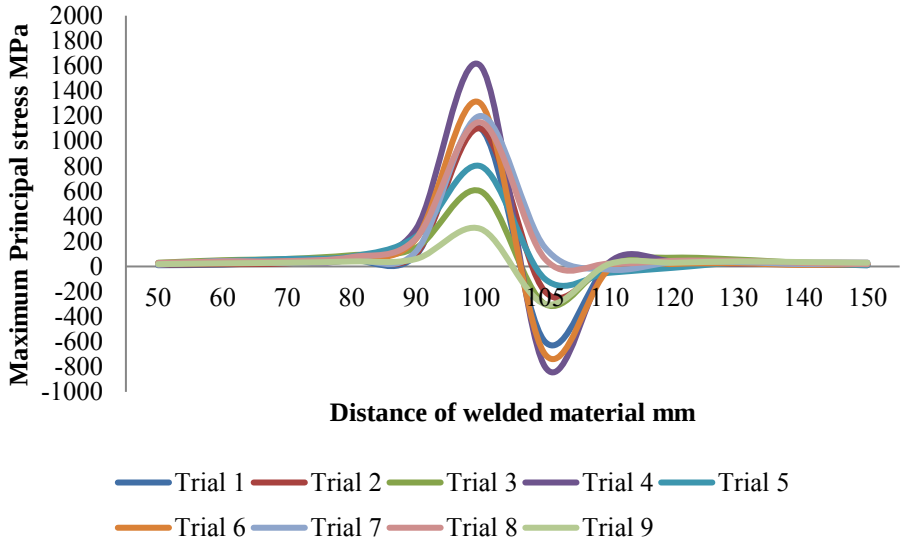

Fig 23. Weld rod joined with maximum stress and different trials

Two dissimilar weld joints are connected with help of ansysworkbench with different trials. These trials results are explained combined stresses are shown in fig 23. Distance and maximum stress results are showed to identify the good bonded strength of weld samples. In this stage of weld process identified trial 7 is the bestto sample of getting well-bonded structures. The sixth set of boundary values are friction pressure is 70 (MPa), friction time is 5 (sec), forging pressure is 70 (MPa), friction time is 5 (sec), speed 2200 (RPM) getting a perfect joint of dissimilar materials of titanium and stainless steel.

5. Conclusion

In this examination work demonstrates acceptable of grating welding procedure of different materials for titanium (Ti-6AL-4V) and treated steel (SS304L) [16]. In this examination work conducts six diverse limit conditions and seven quantities of preliminaries. The CFD results limit conditions are transformed from the underlying qualities. The 6th arrangements of limit conditions are provided a great obligation of joint and less vitality misfortune. The CFD frictional parameters results are contact weight is 70 (MPa), grinding time is 5 (sec), manufacturing weight is 70 (MPa), erosion time is 5 (sec), speed 2200 (RPM). These limit setup results give better sliding contact and great mechanical holding. The stress-life factor results are indicating typical circulation of CFD temperature inclinations. It is prescribed warmth treatment process must degreased time and temperature distributions. The fisher's proportion decrease esteems are 43.8% from the first qualities. Computational fluid dynamics results are carried from the Ansys software identified the heat loss and energy saves in this project.

Reference:

[1] PandiaRajan, S., Senthil kumaran, S., & Kumaraswamidhas, L. A. (2016). An investigation on thermal and friction effect produced by friction welding of SA 213 tube to SA 387 tube plate. Alexandria Engineering Journal, 55(1), 101–112. doi:10.1016/j.aej.2015.12.030

[2] Chennakesava Reddy, A. (2017). Evaluation of Parametric Significance in Friction Welding Process of AA1100 and Zr705 Alloy using Finite Element Analysis. Materials Today: Proceedings, 4(2), 2624–2631. doi:10.1016/j.matpr.2017.02.136

[3] Asif. M, M., Shrikrishana, K. A., &Sathiya, P. (2015).Finite element modelling and characterization of friction welding on UNS S31803 duplex stainless steel joints. Engineering Science and Technology, an International Journal, 18(4), 704–712. doi:10.1016/j.jestch.2015.05.002

[4] Kahveci, K., Can, Y., &Cihan, A. (2005). Heat Transfer in Continuous-Drive Friction Welding of Different Diameters. Numerical Heat Transfer, Part A: Applications, 48(10), 1035–1050. doi:10.1080/10407780500283291

[5] Qinghua, L., Fuguo, L., Miaoquan, L., Qiong, W., & Li, F. (2006). Finite Element Simulation of Deformation Behavior in Friction Welding of Al-Cu-Mg Alloy.Journal of Materials Engineering and Performance, 15(6), 627–631.doi:10.1361/105994906x150821

[6] JI, S., LIU, J., YUE, Y., LÜ, Z., & FU, L. (2012). 3D numerical analysis of material flow behavior and flash formation of 45# steel in continuous drive friction welding.Transactions of Nonferrous Metals Society of China, 22, s528–s533.doi:10.1016/s1003-6326(12)61756-7

[7] Rajesh Jesudoss Hynes, N., Nagaraj, P., Palanichamy, R., Arumugham, C. A. K., & Angela JennifaSujana, J. (2014).Numerical Simulation of Heat Flow in Friction Stud Welding of Dissimilar Metals.Arabian Journal for Science and Engineering, 39(4), 3217–3224.doi:10.1007/s13369-013-0932-3

[8] AYSYS User‘s Manual: _Elements, vol III”, Swanson Analysis Systems, Inc.

[9] Li, X. D., &Wiberg, N. E. (1996). Structural dynamic analysis by a time- discontinuous Galerkin finite element method. International Journal for Numerical Methods in Engineering, 39(12), 2131-2152.

[10] Bendzsak, G. J., North, T. H., & Li, Z. (1997). Numerical model for steady-state flow in friction welding.ActaMaterialia, 45(4), 1735–1745. doi:10.1016/s1359-6454(96)00280-7

[11] D’Alvise, L., Massoni, E., &Walløe, S. J. (2002). Finite element modelling of the inertia friction welding process between dissimilar materials.Journal of Materials Processing Technology, 125-126, 387–391.doi:10.1016/s0924-0136(02)00349-7

[12] Zienkiewicz, O. C., Taylor, R. L., Zienkiewicz, O. C., & Taylor, R. L. (1977). The finite element method (Vol. 36). London: McGraw-hill.

[13] li, Wenya& Shi, Shanxiang& Wang, Feifan& Zhang, Zhihan& Ma, Tiejun& Li, Jinglong. (2012). Numerical Simulation of Friction Welding Processes Based on ABAQUS Environment.Journal of Engineering Science and Technology Review. 5. 10-19. 10.25103/jestr.053.03.

[14] A. Hasçalik, E. Ünal, and N. Özdemir, "Fatigue behaviour of AISI 304 steel to AISI 4340 steel welded by friction welding," Journal of Materials Science, vol. 41, no. 11, pp. 3233–3239, 2006.

[15] Paventhan, R., Lakshminarayanan, P. R., &Balasubramanian, V. (2012). Optimization of Friction Welding Process Parameters for Joining Carbon Steel and Stainless Steel. Journal of Iron and Steel Research International, 19(1), 66–71. doi:10.1016/s1006-706x(12)60049-1

[16] Fomin, A., Egorov, I., Shchelkunov, A., Fomina, M., Koshuro, V., &Rodionov, I. (2018). Composite "1.2361 tool steel – Ti – TiO2" structure and its production by resistance welding with subsequent induction heat treatment. Composite Structures, 206, 467–473. doi:10.1016/j.compstruct.2018.08.084

[17] Ahn, J., He, E., Chen, L., Wimpory, R. C., Dear, J. P., & Davies, C. M. (2017). Prediction and measurement of residual stresses and distortions in fibre laser welded Ti-6Al-4V considering phase transformation. Materials & Design, 115, 441–457. doi:10.1016/j.matdes.2016.11.078

[18] Rajesh Jesudoss Hynes, N., Nagaraj, P., Palanichamy, R., Arumugham, C. A. K., & Angela JennifaSujana, J. (2014).Numerical Simulation of Heat Flow in Friction Stud Welding of Dissimilar Metals.Arabian Journal for Science and Engineering, 39(4), 3217–3224.doi:10.1007/s13369-013-0932-3

[19] Kumar, R & Varatharajan, R & Thiruvengadam, V. (2018). An Investigation of Friction Welding Heat Dissipation in Titanium Alloy and Stainless Steel.International Journal of Ambient Energy.1-10. 10.1080/01430750.2018.1525580.